Supplementary information

Spin-labeled nanobodies as novel protein conformational reporters for EPR in cellular membranes.

Laura Galazzo[1*], Gianmarco Meier[2*], M. Hadi Timachi[1], Cedric A.J. Hutter[2], Markus A. Seeger[2#] and Enrica Bordignon[1#]

Materials and methods

Mutagenesis

To prepare sy- and nanobodies for spin-labeling, cysteine mutations were introduced by QuikChange site-directed mutagenesis. For the sybody, S71C was introduced in Sb_TM#35 using the primers Sb_TM#35_S71C_FW (CAC GGT GTG CCT GGA CAA CG) and Sb_TM#35_S71C_RV (CGT TGT CCA GGC ACA CCG TG). For Nb_TM#1, a cysteine was introduced at position Q44C using the primers Nb_TM#1_Q44C_FW (CTC CAG GGA AGT GCC GCG AG) and Nb_TM#1_Q44C_RV (CTC GCG GCA CTT CCC TGG AG). For Nb_TM#2, a cysteine variant at position S63C was generated with primers Nb_TM#2_S63C_FW (GTA TGC AGA CTG CGT GAA GGG CC) and Nb_TM#2_S63C_RV (GGC CCT TCA CGC AGT CTG CAT AC). Cysteine variants of TM287/288 for spin-labeling have been described in a previous study (1).

Expression and purification of TM287/288

Wild type TM287/288 and the corresponding cysteine mutants were expressed using the pBXNH3L expression vector as described in detail before (2). To generate biotinylated TM287/288, expression vector pBXNH3LCA was used to produce an Avi-tagged version of the transporter as described before in detail (3).

To prepare cysteine mutants of TM287/288 for spin-labeling, 2 mM DTT was included in all buffers during purification. DTT was removed shortly before labeling using a PD-10 column (GE Healthcare) equilibrated with 20 mM Tris-HCl pH 7.5, 150 mM NaCl, and 0.03% (w/v) β-DDM. 10-fold molar excess of MTSL ((1-oxyl-2,2,5,5-tetramethyl-Δ3-pyrroline-3-methyl)methanethiosulfonate, Toronto Research) was added and incubated at 4°C overnight. Wild type TM287/288 and labeled cysteine mutants were finally polished by size-exclusion chromatography using a Superdex 200 Increase 10/300 GL (GE Healthcare) column equilibrated with 20 mM Tris-HCl pH 7.5, 150 mM NaCl and 0.03 % (w/v) β-DDM.

Avi-tagged TM287/288 was enzymatically biotinylated during 3C cleavage with BirA. Biotinylation was performed in 20 mM imidazole pH 7.5, 200 mM NaCl, 10 % (v/v) glycerol, 10 mM magnesium acetate and 0.03 % (w/v) β-DDM with a two-fold molar excess of biotin.

Nanobody and sybody expression and purification

The two nanobodies and the sybody were identified as part of a previous study (3). Single cysteines were introduced at positions S71 (Sb_TM#35), Q44 (Nb_TM#1) and S63 (Nb_TM#2) using site-directed mutagenesis.

Sb_TM#35_S71C and Nb_TM#1_Q44C were expressed from pBXNPHM3 for the production of tag-free binders for DEER experiments (2). In brief, the proteins were produced fused to MBP (Maltose Binding Protein) in the periplasm of *E. coli*, purified under reducing conditions in the presence of DTT, cleaved off from MBP by 3C protease, again purified by reverse IMAC and separated using SEC as described in detail in a previous study (3). Purified Sb_TM#35_S71C and Nb_TM#1_Q44C were stored in 20 mM Tris-HCl pH 7.5, 150 mM NaCl with 2 mM DTT at −80 °C until labeling was performed.

Whereas all nanobodies and sybodies contain a highly conserved disulfide bond at the core of the immunoglobulin domain, Nb_TM#2 features an additional disulfide bond connecting CDR3 with the nanobody framework. Upon reduction, the free thiols of this second disulfide bond are fully accessible for spin-labeling (as opposed to the buried free thiols of the conserved disulfide bond) and consequently, specific spin-labeling of only the newly introduced cysteine was not possible with our standard protocol. Therefore, Nb_TM#2_S63C was purified in the absence of reducing agents. To minimize oxidation of the free cysteine, the purification was performed using degassed buffers at 4°C. In detail, Nb_TM#2_S63C was expressed in the periplasm of *E. coli*

www.pnas.org/cgi/doi/10.1073/pnas.1913737117

using expression vector pBXNPHM3. Freshly transformed *E. coli* MC1061 cells were grown in Terrific Broth (TB) supplemented with 100 µg/mL ampicillin to OD_{600} of 1.0-1.5 at 37°C and expression was induced with 0.02% (w/v) L-arabinose for 16h at 25°C. Cells were harvested and resuspended in 20 mM Tris-HCl pH 7.5, 150 mM NaCl supplemented with DNase (Sigma) and disrupted with an M-110P Microfluidizer® (Microfluidics™). Cell debris were removed by centrifugation at 8,000 g for 1 h and the supernatant was supplemented with 30 mM imidazole, loaded on a Ni-NTA gravity flow column and washed with 20 column volumes 50 mM Imidazole, pH 7.5, 200 mM NaCl and 10% glycerol and eluted with 4 column volumes 200 mM Imidazole, pH 7.5, 200 mM NaCl and 10% glycerol. The eluate was incubated with 3C protease while dialyzing against 20 mM Tris-HCl pH 7.5, 150 mM NaCl overnight at 4°C. Cleaved Nb_TM#2 was reloaded on two Ni-NTA gravity flow columns and eluted with 3 column volumes 20 mM Tris-HCl pH 7.5, 150 mM NaCl and 50 mM imidazole (reverse IMAC). Size exclusion chromatography was performed using a Sepax- SRT10C SEC-300 column (Sepax Technologies) equilibrated with 20 mM Tris-HCl pH 7.5, 150 mM NaCl.

Labeling of binders with Gd-DOTA

For labeling, purified binders were loaded on a PD-10 column (GE Healthcare) equilibrated with degassed PBS pH 7.0 and eluted with 3.2 mL of the same buffer. Binders were labeled at 4°C for 1h with 1.2 molar excess (SbTM#35) or 3.6 molar excess (Nb_TM#1 and Nb_TM#2) of gadolinium-maleimide-DOTA. Samples were then loaded onto a PD-10 column equilibrated with 20 mM Tris-HCl pH 7.5, 150 mM NaCl and eluted with 3.2 mL of the same buffer. Binders were concentrated using Ultra-4 concentrator units with 3kDa MWCO, flash-frozen in liquid nitrogen and stored at −80 °C.

Mass spectrometry analysis of spin-labeled sy- and nanobodies

To determine labeling efficiencies of binders, mass spectrometry was performed on a Synapt-G2 Si mass spectrometer in the range of 50- 5,000 m/z. Capillary voltage was 3.0 kV and the sampling cone energy was set at 40 V. The neutral-mass spectra were inferred from the mass over charge measurement deconvolution using the MaxEnt1 software. Labeling efficiencies were determined based on relative peak heights.

Surface plasmon resonance

Binding affinities were determined with a ProteOn™ XPR36 Protein Interaction Array System (Biorad) at 25°C. ProteOn™ NLC Sensor Chips were loaded with biotinylated TM287/288_E517A^{TM288} to a density of 3,000 RU. SPR measurements were carried out in 20 mM Tris-HCl pH 7.5, 150 mM NaCl, 1 mM MgCl, 0.5 mM ATP and 0.015% (w/v) β- DDM. Measurements were done once and binding affinities calculated using GraphPad Prism assuming 1-to-1 binding.

To determine the binding affinity of Nb_TM#1 to wild type TM287/288 in the absence of ATP-Mg, a Biacore sensor chip CM5 was coated with streptavidin and biotinylated TM287/288 to a density of 2'290 RU. As a control, biotinylated MsbA was coated to a density of 7'630 RU. The SPR measurements were carried out in 20 mM Tris-HCl pH 7.5, 150 mM NaCl with 0.015% (w/v) β- DDM using Nb_TM#1 added at concentrations up to 10 µM. As a control, the measurements were also carried out in the presence of 0.5 mM ATP and 1 mM MgCl.

ATPase assay

ATPase activity was determined using detergent purified TM287/288 at 8 nM in 20 mM Tris-HCl pH 7.5, 150 mM NaCl, 10 mM $MgSO_4$ with 0.03% (w/v) β- DDM. Binders were added at 1 µM (Sb_TM#35 and Nb_TM#1) or 0.2 µM (Nb_TM#2). A non-randomized sybody was added at a concentration of 1 µM and served as negative control. ATPase activities were measured at 25°C for 30 min in the presence of 2 mM ATP. Liberated phosphate was detected colorimetrically using the molybdate/malachite green method. 90 µl reaction solution was mixed with 150 µl filtrated malachite green solution consisting of 10.5 mg/mL ammonium molydate, 0.5 M H_2SO_4, 0.34 mg/mL malachite green and 0.1% Triton X-100. Absorption was measured at 650 nm.

Preparation of inside out vesicles (ISOVs) with overexpressed ABC-transporter

TM287/288 and MsbA were expressed from pBXNH3L. Freshly transformed *E. coli* MC1061 cells were grown in 1 l Terrific Broth (TB) with 100 µg/mL ampicillin to an OD_{600} of 1.0-1.5 at 37 °C. Expression was induced with 0.01 % (w/v) L-arabinose for 1 or 4 hours at 30 °C. Cells were harvested and resuspended in 20 mM Tris-HCl pH 7.5, 150 mM NaCl supplemented with DNase (Sigma). Inside out vesicles were prepared using an M-110P Microfluidizer® (Microfluidics™) at 25'000 psi. Intact cells and cell debris were removed by low spin centrifugation at 8'000 g for 30 min and membranes were collected by high spin centrifugation at 170'000 g for

1,5 h. Inside out vesicles were resuspended in 4 mL 20 mM Tris-HCl pH 7.5, 150 mM NaCl, flash frozen in liquid nitrogen and stored at −80 °C.

EPR experiments

DEER measurements were performed at 50 K (nitroxide-nitroxide) or 10 K (nitroxide-Gd, Gd-Gd) on a Bruker ELEXSYS E580Q-AWG (arbitrary waveform generator) dedicated pulse Q-band spectrometer equipped with a 150 W TWT (Traveling-Wave Tube) amplifier. A 4-pulse DEER sequence with Gaussian (4), non-selective observer and pump pulses of 32 ns length (corresponding to 13.6 ns FWHM, full width at half maximum) with 100 MHz frequency separation was used for NO-NO and Gd-Gd measurements; in the case of Gd-NO measurements, pump pulses of 24 ns length (10.2 ns FWHM) were used in combination with 32 ns observer pulses, with 280 MHz separation between pump and observer. DEER experiments were performed using the dead-time free 4-pulse DEER sequence $(\pi/2)_{obs}$-(d1)-$(\pi)_{obs}$-(d1+T)-$(\pi)_{pump}$-(d2-T)-$(\pi)_{obs}$-(d2)-(echo) with 16-step phase cycling. For the Gd-Gd measurements, we found that a small zero-time artefact due to pulses overlap could be removed by using a 10dB attenuation in the general attenuator. Experimental details regarding the pump and observer positions in the different experiments are given in Fig. S15, while Fig. S16 shows, as an example, two echo decays in detergent and in ISOVs, respectively, for the wild type transporter in the presence of ATP and Nb_TM#1 and Nb_TM#2, both labeled with gadolinium-maleimide-DOTA. The evaluation of the DEER data was performed using DeerAnalysis2019 (4). Interspin distance simulations were performed with the software MMM2018 (5) using the MTSL and Gd-DOTA ambient temperature library.

For DEER measurements, 10% (v/v) glycerol-d8 was added as cryoprotectant to all samples. The final concentration of the detergent-solubilized spin-labeled transporter was 25 µM, of the wild type unlabeled transporter 5 µM. 40 µL of sample was loaded in quartz tubes with 3 mm outer diameter. The ATP-EDTA samples in detergent contained 2.5 mM ATP and 2.5 mM ethylenediaminetetraacetate (EDTA) to completely inhibit ATP hydrolysis; samples were incubated at 25 °C for 8 minutes and snap-frozen in liquid nitrogen. For vanadate trapping, samples were incubated with 5 mM sodium orthovanadate, 2.5 mM ATP and 2.5 mM $MgCl_2$ for 3 min at 50 °C and snap-frozen in liquid nitrogen. For DEER measurements under turnover conditions, 2.5 mM ATP and 2.5 mM $MgCl_2$ were added to the sample and snap-frozen in liquid nitrogen. The two nanobodies were added to the TM287/288 in 1.2:1.2:1 stoichiometric ratio, if not elsewhere specified.

The ISOVs were incubated with 6 µM (for the 4 h overexpression first batch) or 2 µM (for the 1 h overexpression second batch) final concentration of both nanobodies in the absence or presence of 2.5 mM ATP-EDTA. For the washing procedure of the ISOVs, 100 µL of vesicles containing an excess of Gd-labeled Nb_TM#1 and Nb_TM#2 (10 µM for the first batch and 15 µM for the second batch) were diluted to double the volume in buffer alone (apo state) or in a final 2.5 mM concentration of ATP-EDTA (ATP-EDTA state). After ultracentrifugation at 120,000 g and removal of the supernatant, the pellet was resuspended in 300 µL of the same buffer, centrifuged again and resuspended in 35 µL of buffer. 10% (v/v) glycerol-d8 was added as cryoprotectant before freezing of the samples for DEER measurements.

All data presented in the paper will be made available to readers upon request.

	Sb_TM#35		Nb_TM#1		Nb_TM#2	
	K_D [nM]	R_{max} [RU]	K_D [nM]	R_{max} [RU]	K_D [nM]	R_{max} [RU]
unlabeled	130 ± 9	344 ± 8	6.3 ± 0.4	158 ± 2	2.1 ± 0.2	204 ± 4
Gd-labeled	119 ± 10	194 ± 5	7.2 ± 0.4	108 ± 2	1.4 ± 0.3	88 ± 4

Table S1 Binding affinities determined by SPR of unlabeled and Gd-labeled binders SbTM#35, Nb_TM#1 and Nb_TM#2 to TM287/288_E517A^{TM288} in the presence of ATP-Mg.

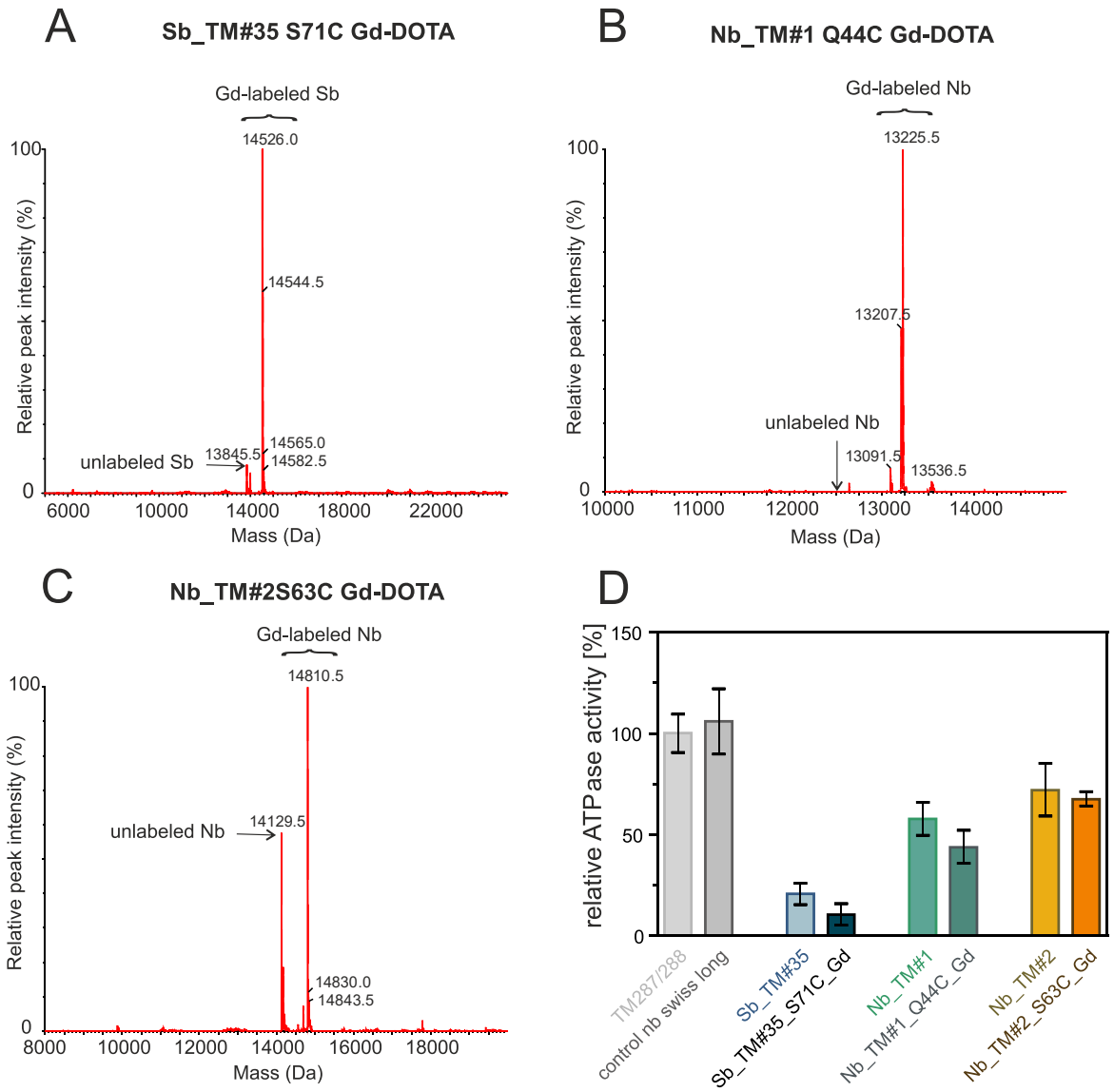

Fig. S1: Mass spectrometry analysis and ATPase activity for the different nanobodies. Mass spectrometry analysis of Sb_TM#35_S71C (A), Nb_TM#1_Q44C (B) and Nb_TM#2_S63C (C) labeled with gadolinium-maleimide-DOTA (Gd-DOTA, expected mass shift upon labeling of 681 Da). The peaks of the labeled and unlabeled binders are marked. In case of the Gd-DOTA labeled Sb_TM#35 (A) and Nb_TM#1 (B), two peaks with a mass deviation of 18 Da are visible. The heavier mass peak corresponds to a water adduct. Based on the peak intensities, the labeling efficiencies were estimated as follows: Sb_TM#35_S71C: 95%, Nb_TM#1_Q44C: 100%; Nb_TM#2_S63C: 65%. (D): Relative ATPase activity of TM287/288 with unlabeled and Gd-labeled binders. A non-randomized sybody was included as a control.

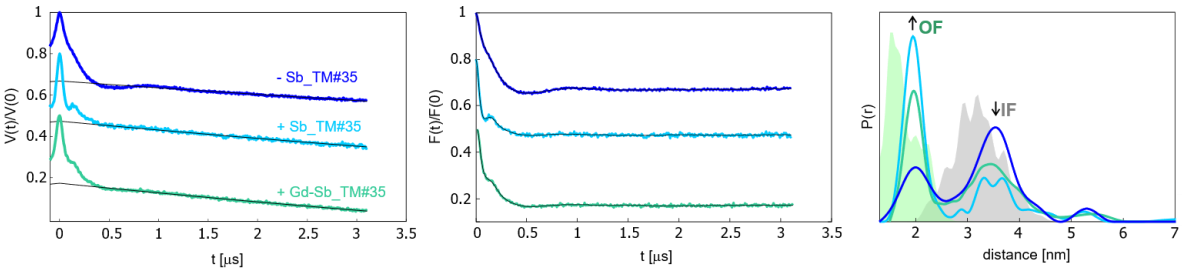

Fig. S2: Conformational equilibrium of TM287/288 in the ATP-bound (ATP-EDTA) state. Nitroxide-nitroxide DEER on the intracellular pair 131^{TM288}/248^{TM288} in the absence of Sb_TM#35 (blue), in the presence of the unlabeled variant (cyan) and of the Gd-labeled variant (turquoise). Left panel: Primary Q-band DEER data; middle panel: background-corrected data; right panel: distance distributions normalized by area. MMM predictions based on the outward-facing (OF) crystal structure (PDB file: 6QUZ) and the inward-facing (IF) crystal structure (PDB file: 4Q4H) are represented as green and grey areas, respectively. The arrows represent the change in population of the IF and OF states upon addition of the sybody.

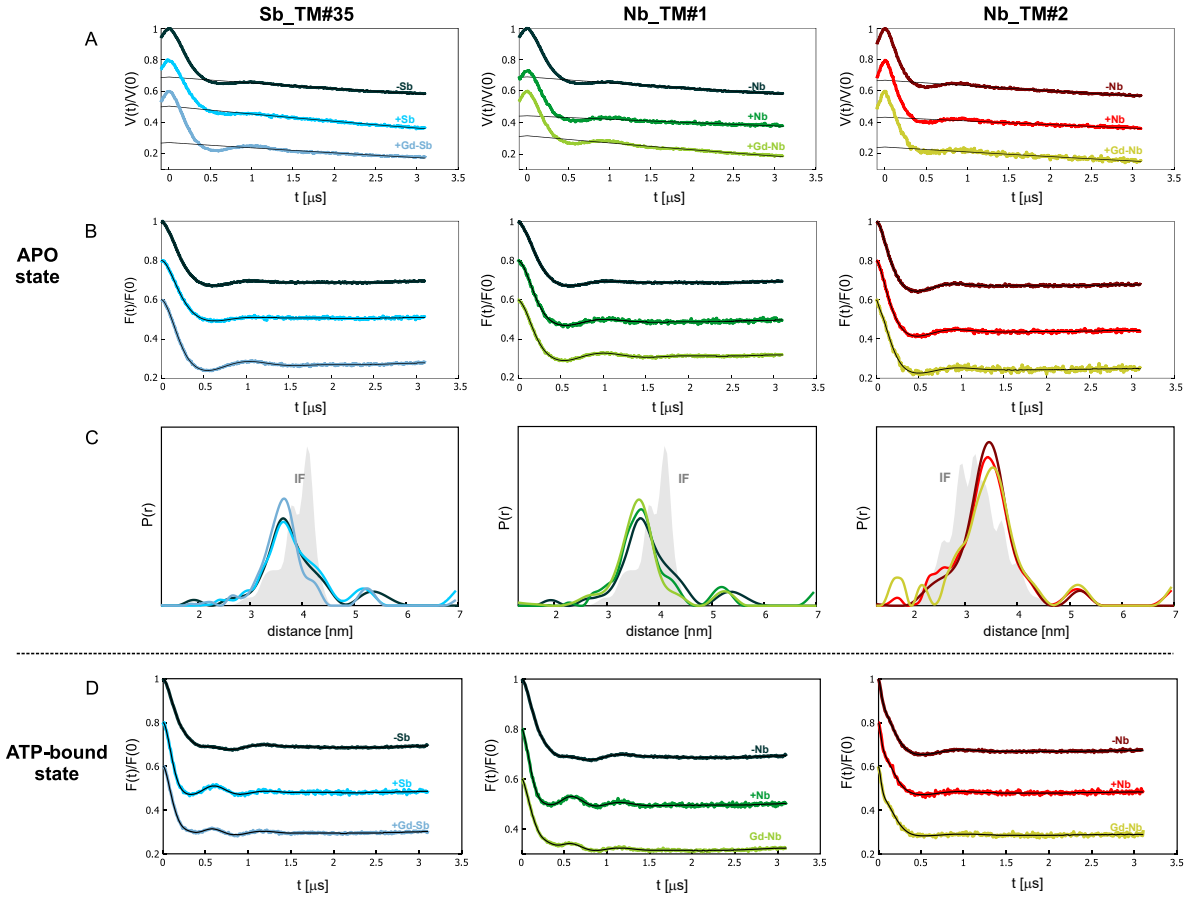

Fig. S3: Comparisons of nitroxide-nitroxide Q-band DEER data in the absence of the different nanobodies (*-Sb/Nb*), in the presence of the unlabeled variants (*+Sb/Nb*) and in the presence of the Gd-labeled variants (*+Gd-Sb/Nb*) in the apo state (A-C) and the ATP-bound (ATP-EDTA) state (D). In the figure, all left panels are referred to Sb_TM#35, all central panels to Nb_TM#1 and all right panels to Nb_TM#2. In the case of Sb_TM#35 and Nb_TM#1, the TM287/288 pair 460^{TM287}/363^{TM288} labeled with MTSL has been investigated. For Nb_TM#2 the spin-labeled TM287/288 pair 131^{TM288}/248^{TM288} has been used due to a steric clash between spin-labeled 363^{TM288} position and Nb_TM#2 (no binding of Nb_TM#2 to spin-labeled 460^{TM287}/363^{TM288} mutant). (A): Primary DEER traces. (B) Background-corrected traces. (C): Distance distributions normalized by area. MMM predictions based on the IF

crystal structure (PDB file: 4Q4H) are represented as grey areas. (D): Background-corrected DEER traces for the data shown in Fig. 2 in the main text.

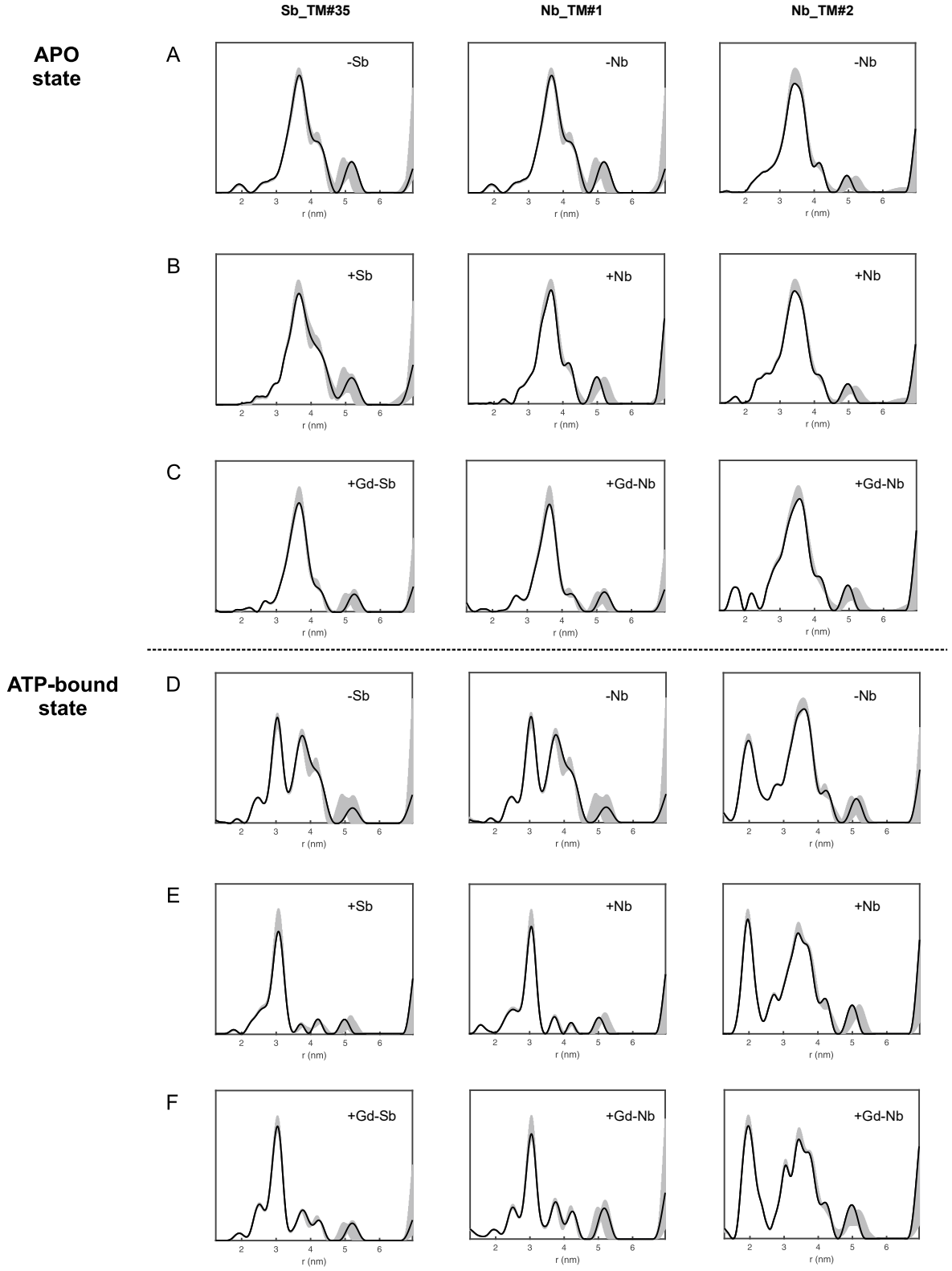

Fig. S4: DeerAnalysis validations of nitroxide-nitroxide Q-band DEER data of Fig. 2 and S3 in the absence of the different nanobodies (-*Sb/Nb*) (A,D), in the presence of the unlabeled variants (+*Sb/Nb*) (B,E) and in the presence of the Gd-labeled variants (+*Gd-Sb/Nb*) (C,F) in the apo state (A-C) and the

ATP-bound (ATP-EDTA) state (D-F). In the figure, all left panels refer to Sb_TM#35, all central panels to Nb_TM#1 and all right panels to Nb_TM#2. Data validation was performed by varying the starting value of the background fit by ±50% in 10 steps and the background dimensionality in 10 steps by ±0.5 relative to the value chosen for the data analysis. The validation tool calculates, for each set of parameters, a distance distribution and performs a statistical analysis. The distance distribution with smallest root-mean-square deviation from the calculated set is shown in black. An uncertainty estimation is given by grey bars, representing the full variation of all calculated distance distributions.

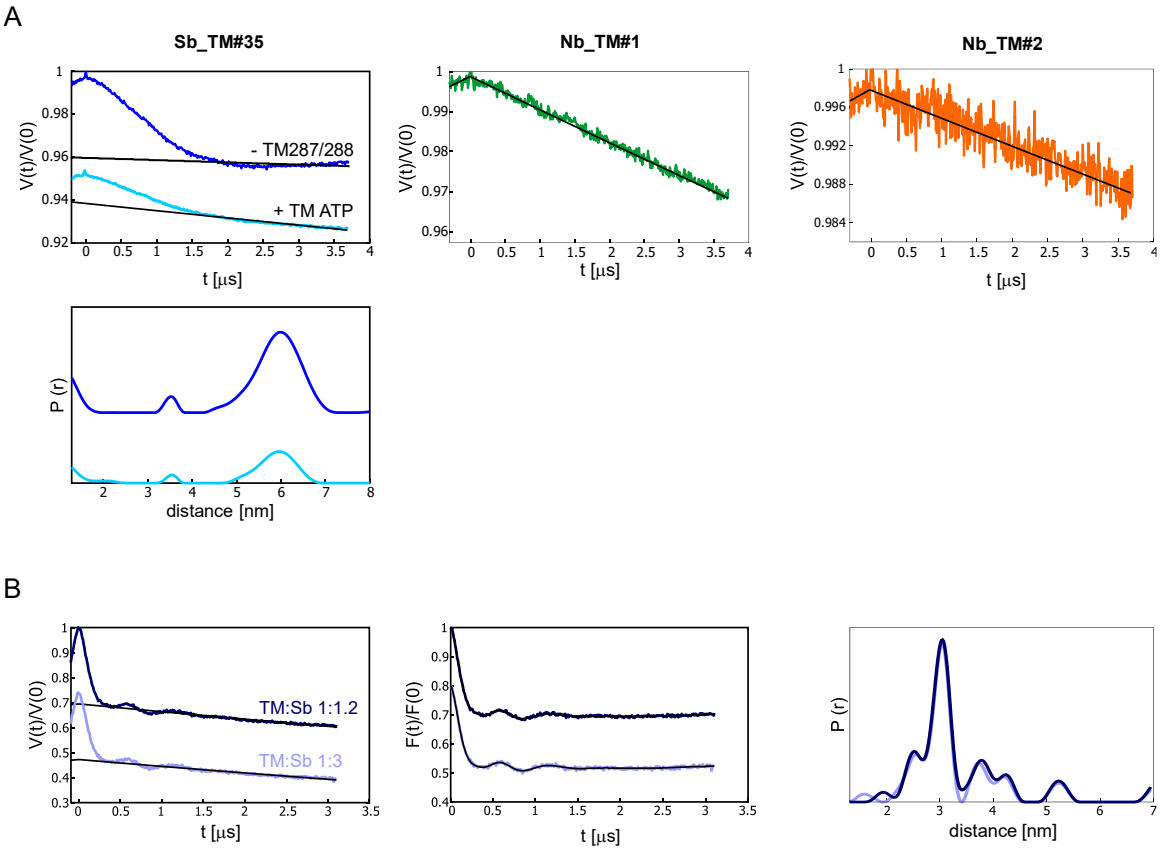

Fig. S5: Dimerization analysis of sy- and nanobodies. (A) Primary Q-band DEER data for the three Gd-labeled sy- and nanobodies in detergent. Sb_TM#35 (left panel, top) dimerizes in the absence of TM287/288 (blue) giving a distance between the two spin labels of about 6 nm (left panel, bottom); in the presence of unlabeled wild type TM287/288 and ATP (+ TM ATP, i.e. when the sybody is bound to the transporter) a substantial proportion of the sybody dimers disappear, as can be seen from the decrease in modulation depth (light blue). Nb_TM#1 and Nb_TM#2 (middle and right panel respectively) do not dimerize under identical experimental conditions. (B) Nitroxide-nitroxide Q-band DEER data for TM287/288 labeled at the NBDs ($460^{TM287}/363^{TM288}$) with MTSL in the presence of ATP-EDTA and Gd-labeled Sb_TM#35 added at different protein/sybody ratios. Left: primary data; middle: background-corrected data; right: distance distributions. Addition of a large excess of the sybody does not alter the conformational equilibrium of the transporter.

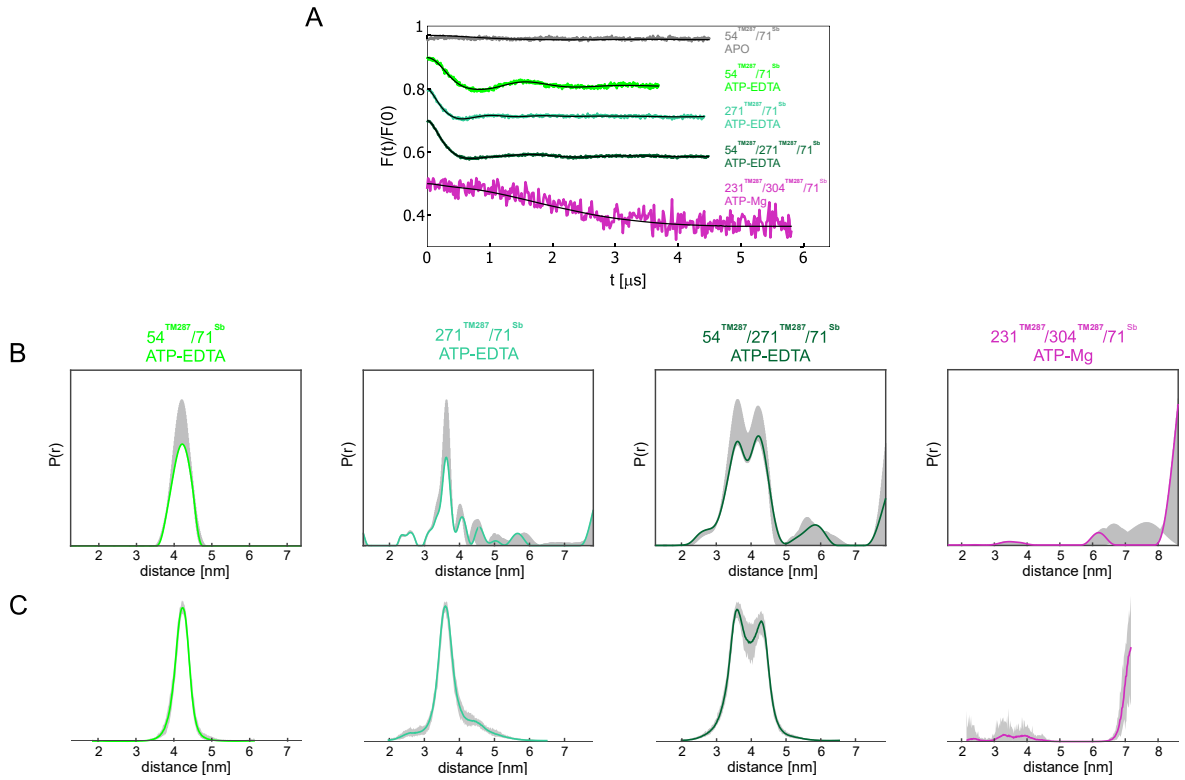

Fig. S6: Form factors and error estimations related to main Fig.3. For each sample, TM287/288 was labeled at one or two different positions with MTSL, while Sb_TM#35 (*Sb*) was labeled at position 71 with Gd-maleimide-DOTA. (A): Background-corrected gadolinium-nitroxide Q-band DEER data. (B): Tikhonov regularization analysis for the different samples and data validations (see Fig. S4 for details regarding the parameters used in the validations). (C): Data evaluation and error estimation using DEERNet (6), a newly implemented tool in DeerAnalysis that uses a trained neural network to extract distance distributions. The two different analyses and their error estimations prove the reliability of the distance information content and show the experimental limit of the analysis on the long distance (relative to the triad 231^{TM287}-304^{TM288}-71^{Sb}), for which the trace is too short to extract a reliable distance information.

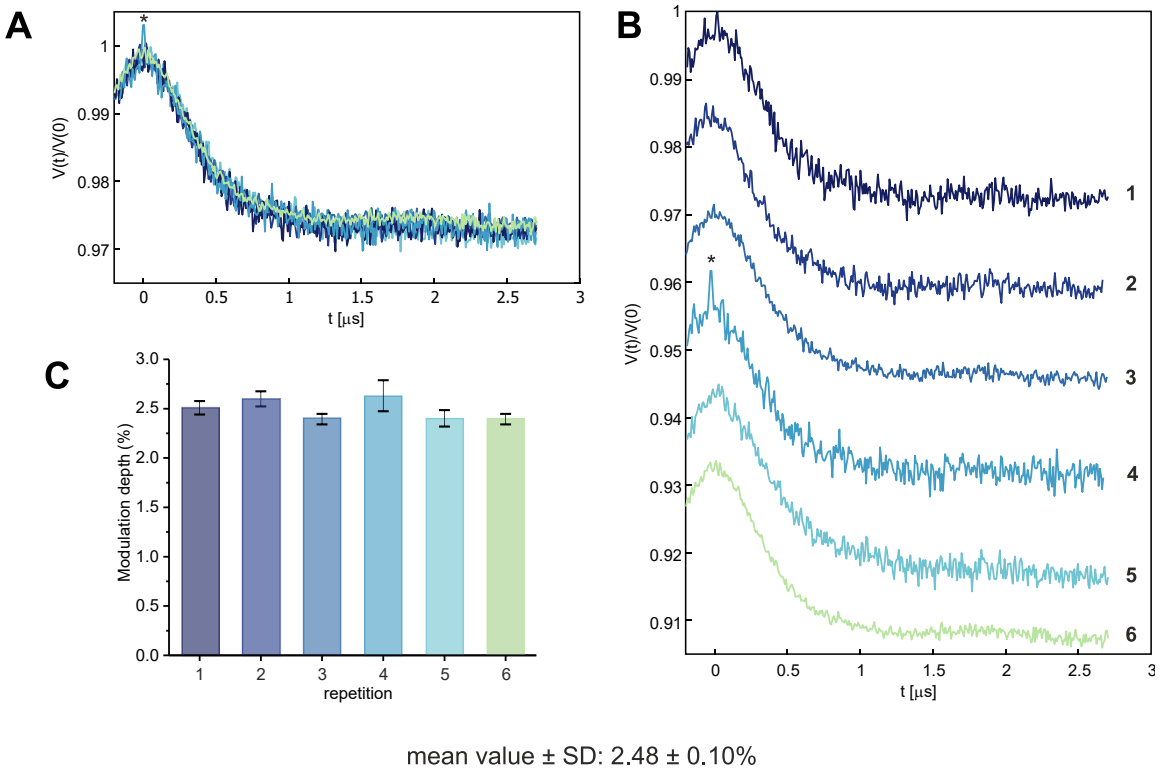

Fig. S7: Statistical analysis of the modulation depths for the Gd-Gd DEER of TM287/288 WT in the presence of ATP-EDTA and Nb_TM#1 and Nb_TM#2 labeled with Gd-maleimide-DOTA in detergent. The six measurements include repetitions on the same DEER tube (samples 3 and 5), on different tubes prepared from different aliquots of the same batch (samples 1, 4 and 6) and on a different batch of nanobodies (sample 2). (A): Primary DEER data for the six repetitions used for the statistical analysis, normalized to the maximum. A y-offset was introduced for better visualization of a zero-time artifact (asterisk) on repetition 4. In panel (B) the same traces are plotted separately. (C): Histograms representing the modulation depths for the different repetitions, together with the errors estimated by DeerAnalysis according to the signal-to-noise ratio. For repetition number 4 the intensity of the zero-time artefact was taken into account in the error estimation. The mean value together with its standard deviation is given. For the determination of the modulation depths, all traces have been analyzed using the same starting point (1000 ns) for the fit of the monoexponential background function. The same fitting procedure was applied to all traces presented in the main figures.

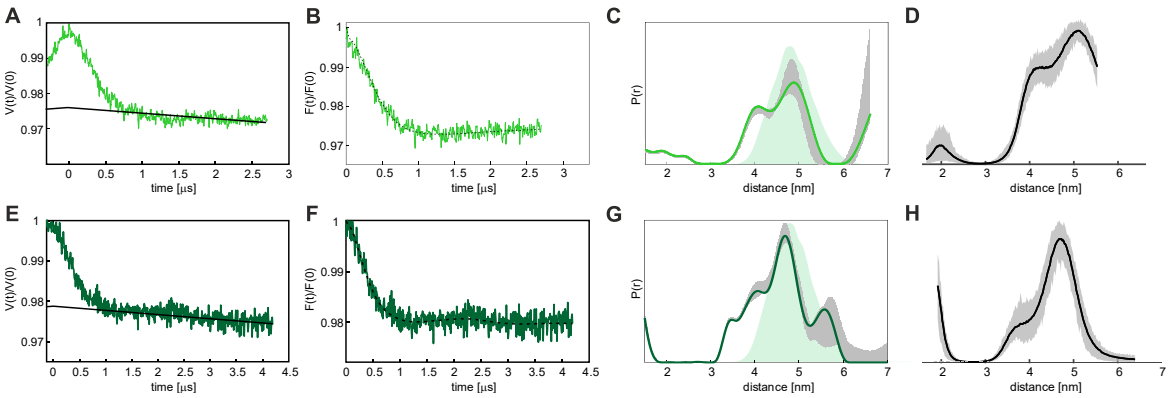

Fig. S8: Validation of the Gd-Gd distance distribution. Short (3 µs d_2 time in the DEER sequence, panels A-D) and long (4.5 µs, panels E-H) traces were recorded using wild type TM287/288 in the presence ATP-EDTA and Nb_TM#1 as well as Nb_TM#2 labeled with Gd-maleimide-DOTA. Primary data (A and E), form factor (B and F) and distance distribution (C and G) are reported. Data were analyzed using Tikhonov regularization and validated with the tools available in DeerAnalysis (grey histogram showing

the uncertainties). For the parameters used in the validations, see the legend of Fig. S4. The green filled curve represents the distances predicted from MMM. In the panels D and H a comparison with DEERNet is shown together with its error estimation. The longer averaging time required in comparison to a shorter trace resulted in a smaller modulation depth, probably due to phase instabilities that may occur over time. As the modulation depth was the important observable for the study, we decided to keep the length of the trace at 3 µs, in order to have a good signal-to-noise ratio with short averaging time (around 1 hour).

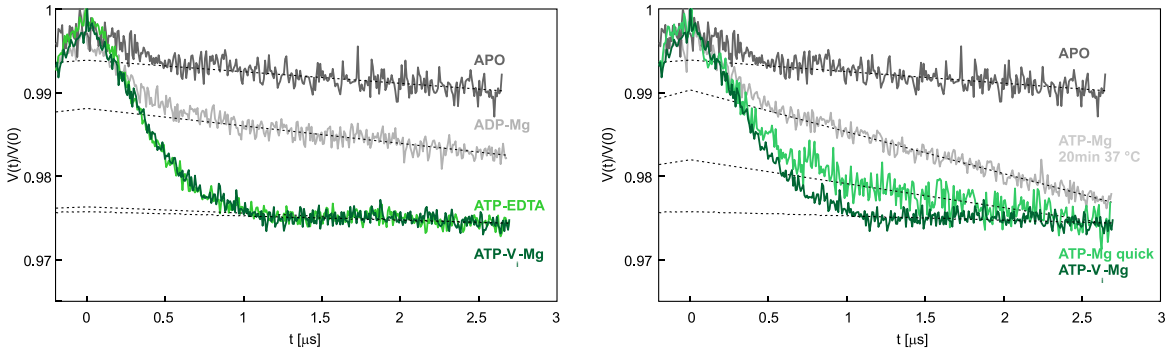

Fig. S9: Primary Q-band DEER data for the measurements shown in the main text in Fig. 4 (left) and Fig. 5 (right) respectively. For the ATP-Mg sample, the zero time has been taken one point after the maximum to minimize the influence of the zero-time artefact in the determination of the modulation depth.

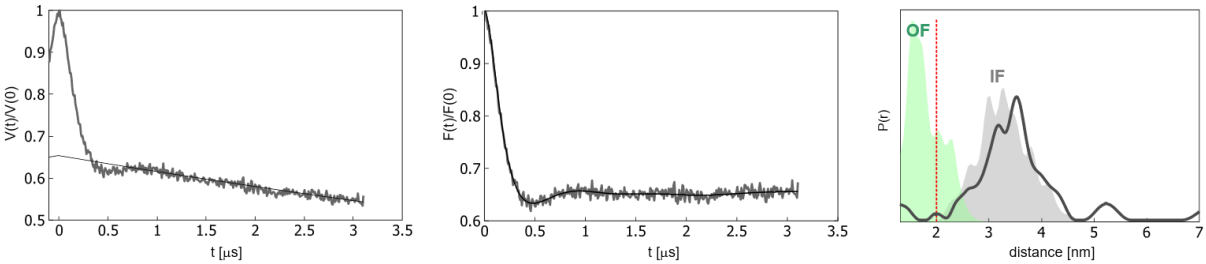

Fig. S10: Nitroxide-nitroxide Q-band DEER data of spin-labeled TM287/288 131^{TM288}/248^{TM288} in the absence of ATP (apo state) and in the presence of Nb_TM#1 and Nb_TM#2. Left panel: Primary Q-band DEER data at 50K; middle panel: background-corrected data; right panel: distance distributions normalized by area. MMM predictions based on the outward-facing (OF) crystal structure (PDB file: 6QUZ) and the inward-facing (IF) crystal structure (PDB file: 4Q4H) are represented as green and grey areas, respectively. The red dashed line represents the main experimental interspin distance of the outward-facing conformation when both nanobodies are present. This control measurement rules out the possibility that a measurable fraction of OF state is present in the presence of Nb_TM#1 and Nb_TM#2.

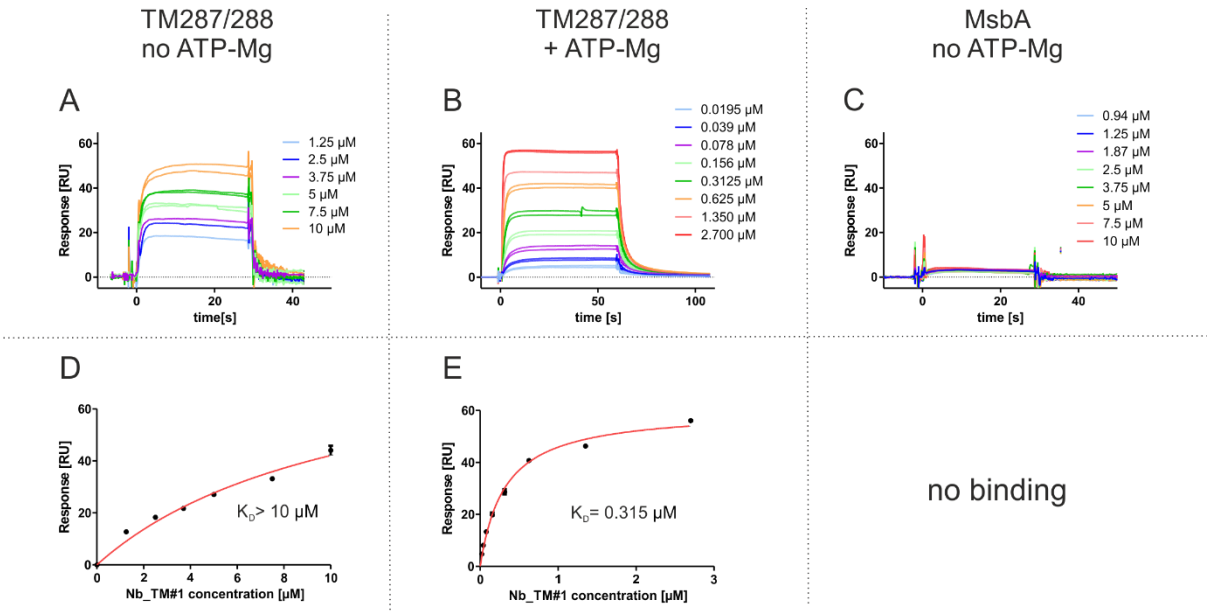

Fig. S11: Determination of binding affinity of Nb_TM#1 to TM287/288 . (A-C) SPR traces using wild type TM287/288 (A and B) as well as MsbA (C) as ligands and Nb_TM#1 as analyte at the concentrations indicated in the graphs. Measurements were conducted in the absence (A and C) or presence of ATP-Mg (B). (D and E) Equilibrium binding signals measured in (A and B) were plotted against the injected Nb_TM#1 concentration. K_D values were determined by fitting the data using a hyperbolic equation. The K_D for Nb_TM#1 against apo TM287/288 could not be reliably determined based on these SPR analyses (D), and was estimated to be greater than 10 µM.

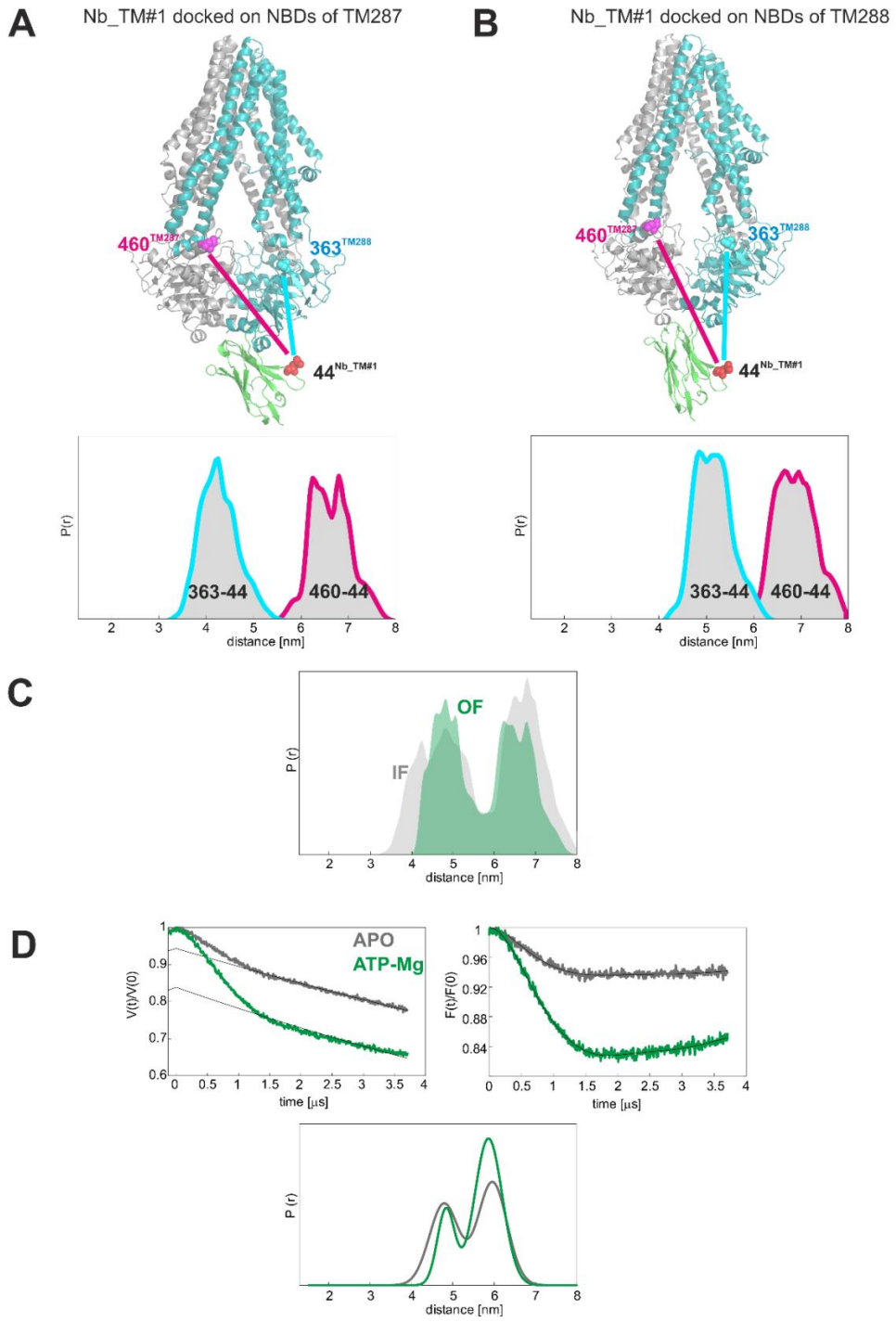

Fig. S12: Possible conformations of Nb_TM#1 bound to the inward-facing state of the transporter. The binding epitope of the nanobody is shared between the NBDs of TM287 and TM288, therefore, starting from the crystal structure of the apo state (PDB file: 4Q4H) two independent dockings are possible, at the two different NBDs. In (A), the docking of Nb_TM#1 to TM287 is shown, while in (B) the corresponding one to TM288 is presented. At the bottom of each docking model, the MMM predictions for the NO-Gd distances between the pair 460^{TM287}-$44^{Nb\_TM\#1}$ (magenta) and 363^{TM288}-$44^{Nb\_TM\#1}$ (cyan) are displayed. The sum of the four distance distributions is given in (C) as grey area. The corresponding NO-Gd distances simulated with MMM for the triad 460^{TM287}-363^{TM288}-$44^{Nb\_TM\#1}$ in the outward-facing state are shown as a green area. The distance distributions in the two different conformations are so similar that they cannot be experimentally distinguished. (D): DEER measurements on the double mutant 460^{TM287}-363^{TM288} in the E-to-Q variant (chosen to block ATP hydrolysis) labeled with MTSL in the presence of Nb_TM#1 (20 µM) labeled with Gd-maleimide-DOTA shows a residual dipolar

modulation in the apo state for the Gd-NO channel, confirming its binding to the apo state, in line with the SPR data and with the data obtained when both Gd-labeled nanobodies were bound to the wild type transporter. In the presence of ATP-Mg, the modulation depth increases by three-fold; the same ratio was found in the Gd-Gd measurements between the two nanobodies in the wild-type protein (see Fig. 4), which highlights the reliability of the data extracted via modulation depth.

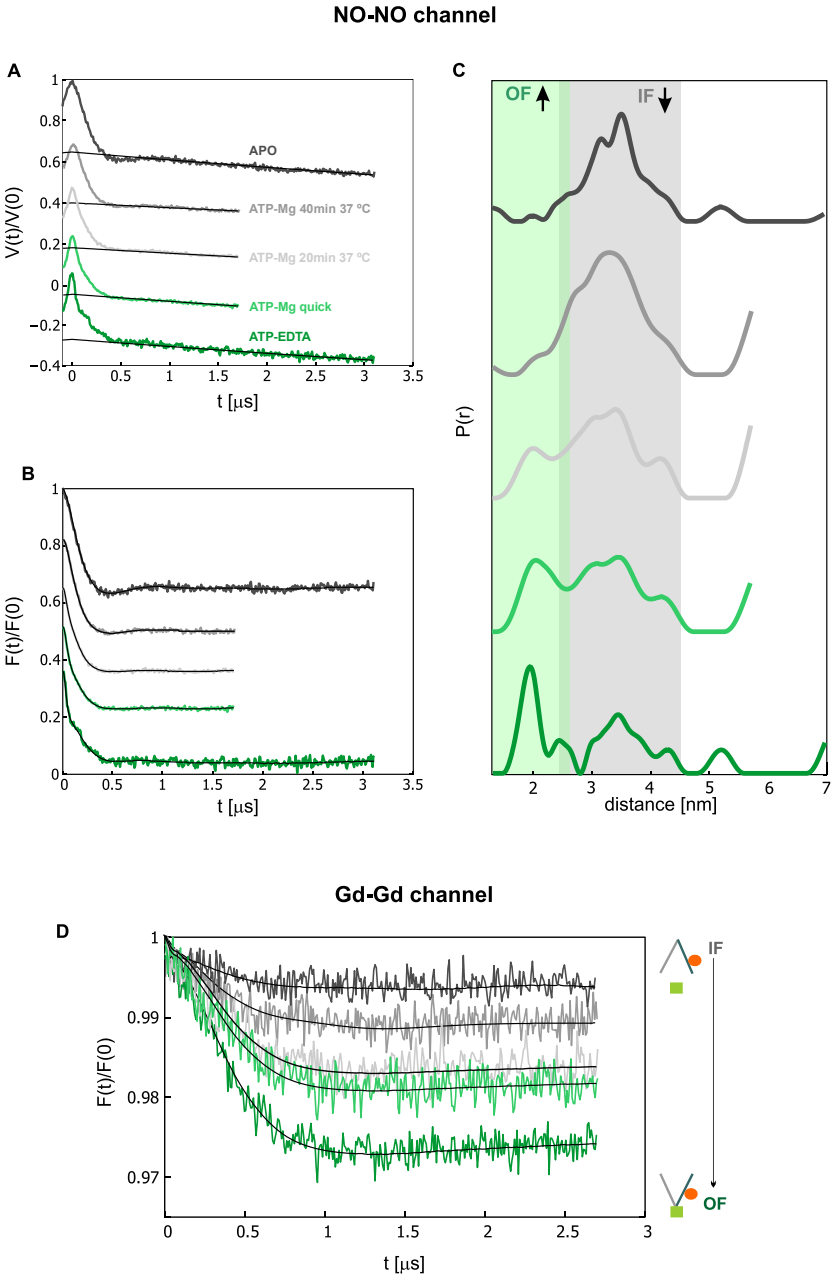

Fig. S13: Nitroxide-nitroxide and gadolinium-gadolinium DEER data on the intracellular pair $131^{TM288}/248^{TM288}$ (labeled with MTSL) in different states of the ATP cycle in the presence of Nb_TM#1 and Nb_TM#2 6 µM each (labeled with Gd-maleimide-DOTA). (A): Primary nitroxide-nitroxide Q-band DEER data; (B): background-corrected DEER traces; (C): distance distributions normalized by area. The green and grey rectangles represent the predicted interspin distance in the OF and IF states, respectively; (D): background-corrected DEER traces for the same samples when the Gd-Gd DEER channel is monitored. The increasing fraction of OF state detected in the NO-NO DEER channel correlates with the increase in the modulation depth of the traces recorded in the Gd-Gd DEER channel.

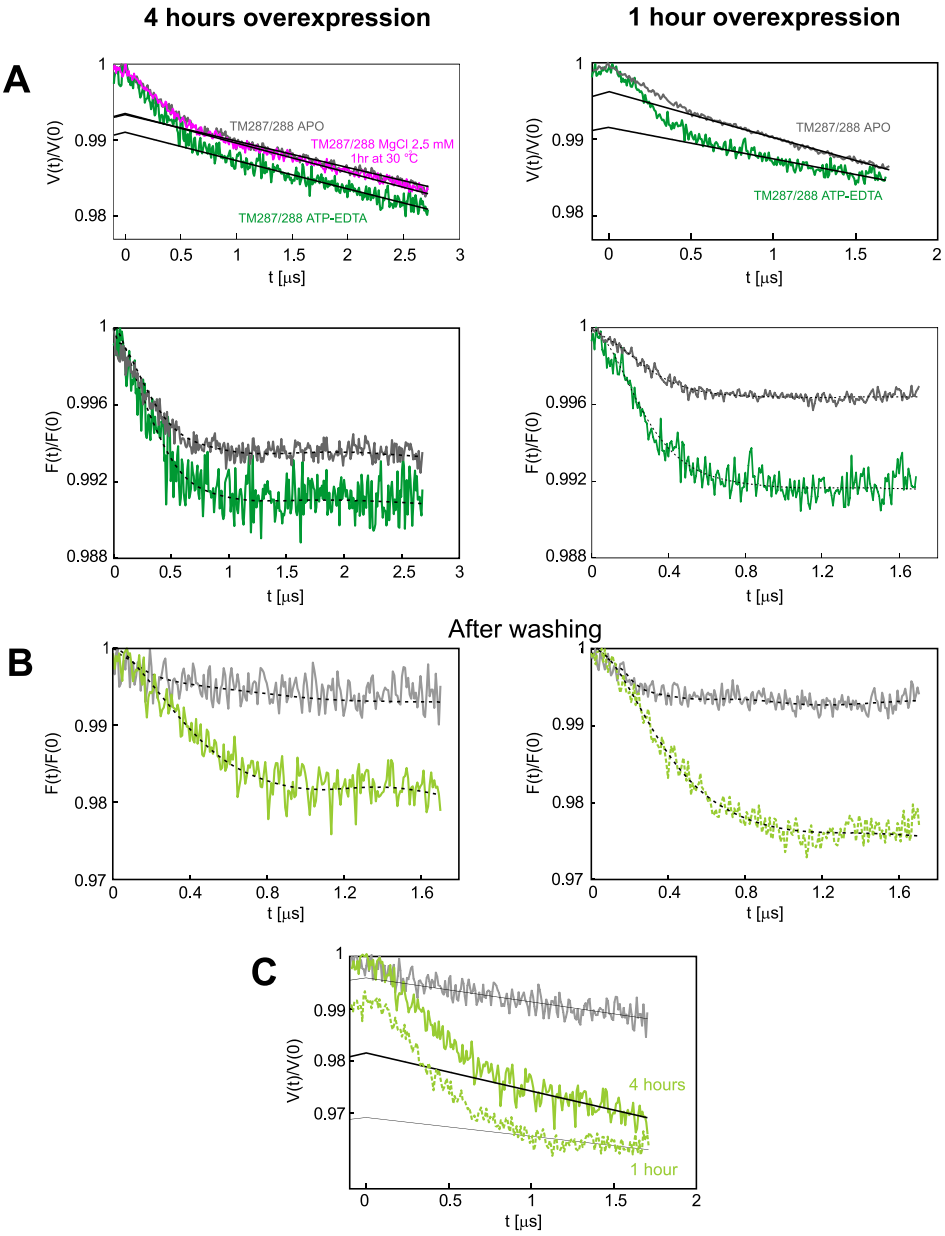

Fig. S14: Q-band DEER on wild-type TM287/288 in the presence of Nb_TM#1 and Nb_TM#2 in inside-out vesicles at different overexpression levels. (A): Upper panels: Primary DEER traces of the ISOVs with different overexpression levels: four hours (left) and one hour (right) (apo: grey and ATP-EDTA: green). The trace collected after one-hour incubation with 2.5 mM $MgCl_2$ to fully hydrolyze residual ATP that may have been carried over from the ISOVs preparation is shown in magenta. Lower panels: background-corrected data. (B): Background-corrected data of the washed ISOVs with different overexpression levels: four hours (left) and one hour (right, related to Fig. 6B) (apo: grey and ATP-EDTA: light green). (C) Primary DEER traces of the ISOVs after four hours overexpression (solid lines, related to panel B, left) compared with the primary trace of the ATP-EDTA state (one-hour overexpression) presented in Fig. 6B (light green, dotted). This comparison highlights the increased background steepness for the membranes with higher protein expression level.

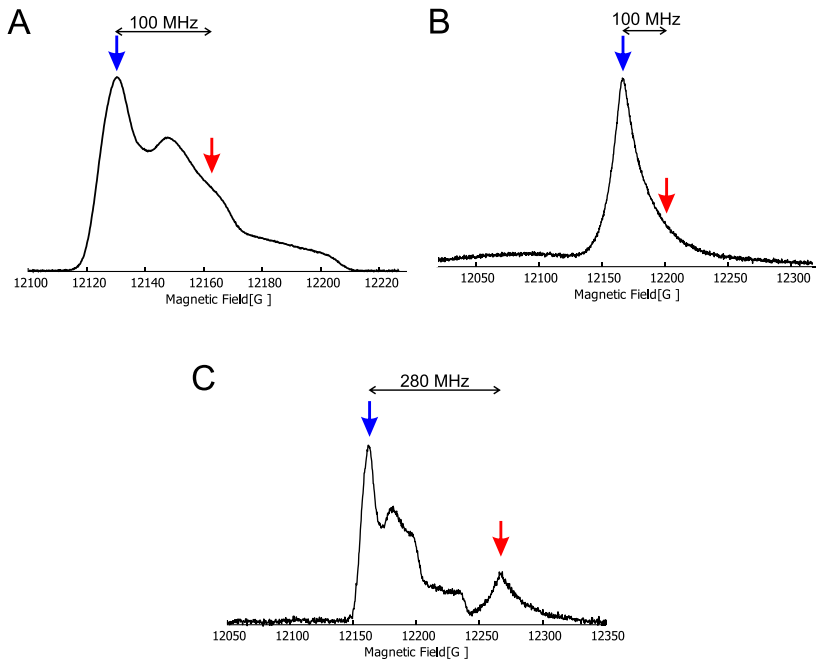

Fig. S15: Experimental details on DEER performed on different channels. The panels represent the three setups used: (A) NO-NO channel, (B) Gd-Gd channel, (C) NO-Gd channel. Examples of field-swept echo experiments are shown for a sample containing a nitroxide (A) recorded at 50 K, Gd-maleimide-DOTA (B) recorded at 10 K and both spin types in the same mixture (C) recorded at 10 K. The field positions at which pump pulses have been set for DEER experiments are highlighted with a blue arrow, while the observer position is indicated with a red arrow. The separation between pump and observer is also specified for the three different experiments. Different sweep widths are shown to better highlight the spectral features.

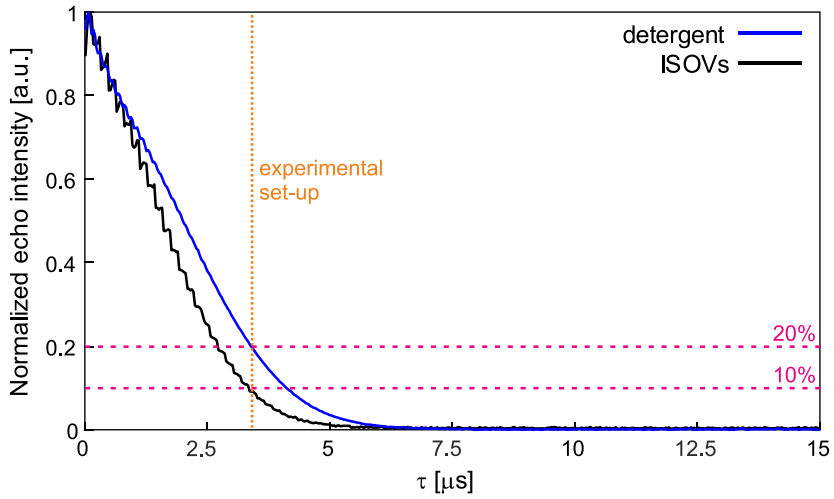

Fig. S16: Echo decay traces measured at 10 K at the maximum of the Gd signal for TM287/288 WT in the presence of ATP-EDTA and Nb_TM#1 and Nb_TM#2 labeled with Gd-maleimide-DOTA in detergent (blue) and in ISOVs (black). The x axis represents the increment (τ) of the 400 ns starting interpulse delay between the $\pi/2$ and π pulses. The orange vertical line shows the length of the dipolar evolution time chosen for the DEER measurements. The magenta horizontal lines represent the residual echo intensity at the experimental conditions. The two-fold higher echo intensity in the detergent sample, compared to the one in ISOVs, implies that the measuring time of a DEER is four times faster in detergent than in ISOVs to reach the same signal-to-noise ratio, as experimentally observed.

References

1. Timachi MH*, et al.* (2017) Exploring conformational equilibria of a heterodimeric ABC transporter. *Elife* 6.
2. Hutter CAJ*, et al.* (2019) The extracellular gate shapes the energy profile of an ABC exporter. *Nature communications* 10(1):2260.
3. Zimmermann I*, et al.* (2018) Synthetic single domain antibodies for the conformational trapping of membrane proteins. *Elife* 7.
4. Jeschke G*, et al.* (2006) DeerAnalysis2006 - a comprehensive software package for analyzing pulsed ELDOR data. *Appl. Magn. Reson.* 30(3-4):473-498.
5. Jeschke G (2018) MMM: A toolbox for integrative structure modeling. *Protein Sci.* 27(1):76-85.
6. Worswick SG, Spencer JA, Jeschke G, & Kuprov I (2018) Deep neural network processing of DEER data. *Sci. Adv.* 4(8):eaat5218.